



**HAL**  
open science

## Effect of Cellulosic Waste Derived Filler on the Biodegradation and Thermal Properties of HDPE and PLA Composites

Alessia Quitadamo, Valérie Massardier, Valeria Iovine, Ahmed Belhadj, Rémy Bayard, Marco Valente

► **To cite this version:**

Alessia Quitadamo, Valérie Massardier, Valeria Iovine, Ahmed Belhadj, Rémy Bayard, et al.. Effect of Cellulosic Waste Derived Filler on the Biodegradation and Thermal Properties of HDPE and PLA Composites. *Processes*, 2019, 7 (10), pp.647. 10.3390/pr7100647 . hal-02417888

**HAL Id: hal-02417888**

**<https://hal.science/hal-02417888v1>**



Submitted on 17 Sep 2024

**HAL** is a multi-disciplinary open access archive for the deposit and dissemination of scientific research documents, whether they are published or not. The documents may come from teaching and research institutions in France or abroad, or from public or private research centers.

L'archive ouverte pluridisciplinaire **HAL**, est destinée au dépôt et à la diffusion de documents scientifiques de niveau recherche, publiés ou non, émanant des établissements d'enseignement et de recherche français ou étrangers, des laboratoires publics ou privés.

Article

# Effect of Cellulosic Waste Derived Filler on the Biodegradation and Thermal Properties of HDPE and PLA Composites

Alessia Quitadamo <sup>1,2</sup>, Valerie Massardier <sup>2</sup>, Valeria Iovine <sup>1</sup>, Ahmed Belhadj <sup>2</sup>, Rémy Bayard <sup>3</sup> and Marco Valente <sup>1,\*</sup>

<sup>1</sup> Department of Chemical and Material Environmental Engineering, Sapienza University of Rome, 00184 Rome, Italy; alessia.quitadamo@uniroma1.it (A.Q.); valeria.iovine@hotmail.it (V.I.)

<sup>2</sup> Ingénierie des Matériaux polymers, Université de Lyon, INSA Lyon, 69621 Villeurbanne, France; valerie.massardier@insa-lyon.fr (V.M.); ahmed.belhadj@insa-lyon.fr (A.B.)

<sup>3</sup> DEEP Laboratory, Université de Lyon, INSA Lyon, 69621 Villeurbanne, France; remy.bayard@insa-lyon.fr

\* Correspondence: marco.valente@uniroma1.it; Tel.: +0644585582

Received: 1 August 2019; Accepted: 12 September 2019; Published: 21 September 2019



**Abstract:** Composites with high density polyethylene (HDPE) and poly(lactic) acid (PLA) matrix have been tested to analyze the effect of natural fillers (wood flour, recycled wastepaper and a mix of both fillers) and temperature on polymer degradation. Composting tests have been performed in both mesophilic (35 °C) and thermophilic (58 °C) conditions. Degradation development has been evaluated through mass variation, thermogravimetric analysis and differential scanning calorimetry. HDPE, as expected, did not display any relevant variation, confirming its stability under our composting conditions. PLA is sensibly influenced by temperature and humidity, with higher reduction of  $M_w$  when composting is performed at 58 °C. Natural fillers seem to influence degradation process of composites, already at 35 °C. In fact, degradation of fillers at 35 °C allows a mass reduction during composting of composites, while neat PLA do not display any variation.

**Keywords:** biodegradation; bio-derived polymer; composites

## 1. Introduction

Degradation is a typical phenomenon of polymer materials leading to fragmentation and significant changes in the structure of the material characterized by the loss of some properties (e.g., mechanical properties, viscosity, molecular weight) [1,2]. Degradation can occur in different ways such as thermal degradation, photo degradation, oxidative degradation, mechanical degradation, hydrolysis reaction with water (hydrolytic degradation) and action of microorganisms such as bacteria, fungi or algae (biodegradation) [3–5].

In general, the degradation pathways associated with polymer degradation are often determined by environmental conditions, depending on aerobiosis (presence of oxygen) or anaerobiosis (absence of oxygen), and it is based on oxidation or hydrolysis reactions [6–8]. These reactions can take place simultaneously or in succession. Anaerobic biodegradation is characterized by three main phases: firstly, hydrolysis occurs, making available molecules for bacteria digestion, secondly acid and acetogenesis convert sugars and amino acids into  $\text{CO}_2$ ,  $\text{H}_2$ ,  $\text{NH}_3$  and acetic acid [9,10]. Finally, methanogenesis produces methane,  $\text{CO}_2$  and water. Macroscopically, biodegradation appears as yellowing, fragmentation and breakage [11]. Aerobic degradation, when  $\text{O}_2$  is available, is characterized by the decomposition of polymers by oxidation which can be followed by hydrolysis of the oxidation products whose final products will be microbial biomass,  $\text{CO}_2$  and  $\text{H}_2\text{O}$ . Biodegradability can be evaluated through several standards, depending on the final application of the tested materials.

Several studies have been performed in order to evaluate biodegradability behavior of bio-derived polymers and composites, or to verify the effect of pro-oxidant on oil-based polymers [12–14]. The purpose of this work is to evaluate the effect of natural fillers on biodegradability of bio-derived and oil-based polymers. In 1993, Sinclair et al. already [15] patented blends of polylactic acids with traditional oil-based polymers, aiming to produce blends with environmentally degradable features. They obtained partially degradable materials, in which poly(lactic) acid (PLA) rapidly decomposed, compared to stable traditional polymers. The interesting aspect is the higher rapidity of degradation of these blends in comparison to conventional non-degradable plastics because of two simultaneous aspects: firstly, PLA degradation occurs, and secondly, this degradation allows the formation of high specific surface area that is expected to accelerate the process. Environmental consciousness has attracted much interest over recent years, directing researches through the use of bio-derived polymers and natural fillers [16–18]. In fact, composites with natural fillers gain great attention during last decades [19–21]. Lignocellulosic fibers are characterized by a chemical composition influenced by genetic and environmental factors. In general, lignocellulosic fibers are mainly composed of cellulose (linear macromolecules of glucose units, the higher the amount of cellulose the higher the hydrophilicity of the fibers), hemicellulose (composed of several polysaccharides) and lignin (irregular and insoluble polymer, composed of aromatic units characterized by highly networked structures) [21,22]. Chemical structure of lignocellulosic fibers directly affects not only mechanical properties, but also biodegradability. In fact, each constituent of lignocellulosic fibers can be more or less susceptible to enzymatic hydrolysis, depending on the particular chemical structure [23]. Generally speaking, biological degradation occurs firstly for hemicellulose, then amorphous cellulose and lastly for crystalline cellulose [24]. In fact, packed structures are less accessible for microorganisms, preventing macromolecule degradation. Biodegradation occurs through breakage of  $\beta$  1,4-xylan bonds of hemicellulose by xylanase,  $\beta$  1,4-glycosidic bonds of cellulose by cellulase and lignin biodegradation thanks to ligninolytic fungi actions.

In our work, samples have been subjected to composting in soil for three months at 35 °C and 58 °C, in order to evaluate their degradation. In particular, HDPE-based and PLA-based composites have been tested to analyze the effect of natural fillers (wood flour, recycled wastepaper and a mix of both fillers) on polymer degradation. Both mesophilic and thermophilic conditions have been tested to also analyze temperature influence on composting processes. Common techniques [25,26] have been used to follow biodegradation over time, such as DSC, TG, FTIR, SEC and mass variation.

## 2. Materials and Methods

### 2.1. Materials

Eraclene MP90, commercial name of high-density polyethylene (HDPE) from ENI (Versalis, Milan, Italy), has been selected as oil-based polymer. Among its properties (derived from datasheet) are: a melt flow index (MFI) of 7 g/10 min (190 °C/2.16 kg), a nominal mass of 0.96 g/cm<sup>3</sup>, a tensile strength of 21 MPa, a tensile modulus of 1.2 GPa, a Shore D hardness of 50. Poly (lactic acid) (PLA) Ingeo Biopolymer 3251D from Nature Works (Blair, NE, USA) was selected as bio-derived thermoplastic polymer, with a MFI of 35 g/10 min (190 °C/2.16 kg). This polymer is characterized by density 1.24 g/cm<sup>3</sup>, crystalline melting temperature in the range 155–170 °C and a glass transition temperature in the range 55–60 °C (derived from datasheet). La.So.Le-est/Srl (Udine, Italy) provided the WF (European beech) with dimensions derived from datasheet: >500  $\mu$ m 0–5%, >300  $\mu$ m 20–70%, >180  $\mu$ m 20–80%, <180  $\mu$ m 0–5%. Recycled wastepaper, whose production process is deeply described in another work [20], have been observed with optical microscopy. Average length of 750  $\pm$  300  $\mu$ m and diameter of 25  $\pm$  10  $\mu$ m have been measured. PLA, WF and recycled wastepaper were dried one night at 80 °C under vacuum, before processing.

A Micro 15 Twin-screw DSM research extruder was used at 180 °C, with screw speed of 75 rpm, N<sub>2</sub> atmosphere and 4 min residence time. The injection molding temperature was 55 °C, and pressure

parameters were dependent on the formulation specificities because of different viscosities. Disks of 40 mm diameters and 1.5 mm thickness have been produced.

## 2.2. Composting Tests

Tests were performed in order to analyze the effect of testing temperature, wood flour (WF) and cellulosic fibers (P) on HDPE and PLA, as well as the behavior of soy protein isolate (with 30% of glycerol as plasticizer), used as positive reference. Tests duration was three months, keeping samples under both mesophilic (35 °C) and thermophilic (58 °C) conditions [27]. Mesophilic condition was obtained, keeping the three aquaria in a thermostatted chamber, while for thermophilic condition three aquaria were put in an oven. In each aquarium, 2 kg of compost were used: 1 kg was put at the bottom, samples were placed and then 1 kg of compost was used to bury samples. During the test, humidity was checked and kept at constant value. Before burying, all samples were dried all night under vacuum at 50 °C and weighted. Table 1 displays all formulations subjected to this test.

**Table 1.** Formulations of samples for composting test in soil.

Samples	High Density Polyethylene HDPE (%)	Poly(lactic) Acid PLA (%)	Wood Flour (WF) (%)	Recycled Wastepaper (P) (%)
HDPE	100			
PLA		100		
HDPE60-WF40	60		40	
HDPE60-P40	60			40
PLA60-WF40		60	40	
PLA60-P40		60		40
PLA60-WF30-P10		60	30	10

Each month a disk per formulation is taken from the aquarium, washed with distilled water and dried until constant weight is reached. The evolution of degradation is analyzed by mass variation of each samples as:

$$\Delta M (\%) = (M_{t0} - M_t) / M_{t0} \times 100$$

In which  $\Delta M (\%)$  is mass variation,  $M_{t0}$  is mass value before composting and  $M_t$  is mass value at time  $t$  (respectively 1, 2, 3 months at 35 °C and 58 °C). Moreover, other tests have been performed to analyze degradation evolution, such as: Thermogravimetric analysis (TGA) carried out on a Q500 Thermal Analysis instrument up to 600 °C with a scanning temperature of 10 °C·min<sup>-1</sup> under a nitrogen flow of 50 mL·min<sup>-1</sup> and Differential scanning calorimetry (DSC) performed on a Q20 Thermal Analysis instrument) with two cycles (with a 4 min interval between them) at 180 °C to eliminate trace of thermal history. The first cycle was carried out from 25 °C to 180 °C under a nitrogen flow of 50 mL·min<sup>-1</sup> followed by a cooling from 180 °C to 25 °C.  $T_c$  and  $\Delta H_c$  were measured during this cooling phase. Then, a second heating from 25 °C to 180 °C enabled a determination.  $T_{cc}$ ,  $T_f$  and  $\Delta H_f$ . All heating scans were performed at 10 °C·min<sup>-1</sup> (Figure 1).

Size Exclusion Chromatography (SEC) was performed using a Shimadzu apparatus) equipped with a refractive index detector (RI) to determine polymer molar masses. The eluent was tetrahydrofuran (THF) with a flow rate of 1 mL/min. Universal calibration was performed using polystyrene standards. Samples were dissolved in THF eluent (around 15 mg samples for 10 mL eluent), and then filtered using PTFE filters of 0.45 µm.

Infrared Analysis Attenuated Total Reflection (ATR-FTIR) tests were carried out with a thermo-scientific Nicolet IS10 spectrometer, with a spectral range 4000–400 cm<sup>-1</sup> and 32 scans.

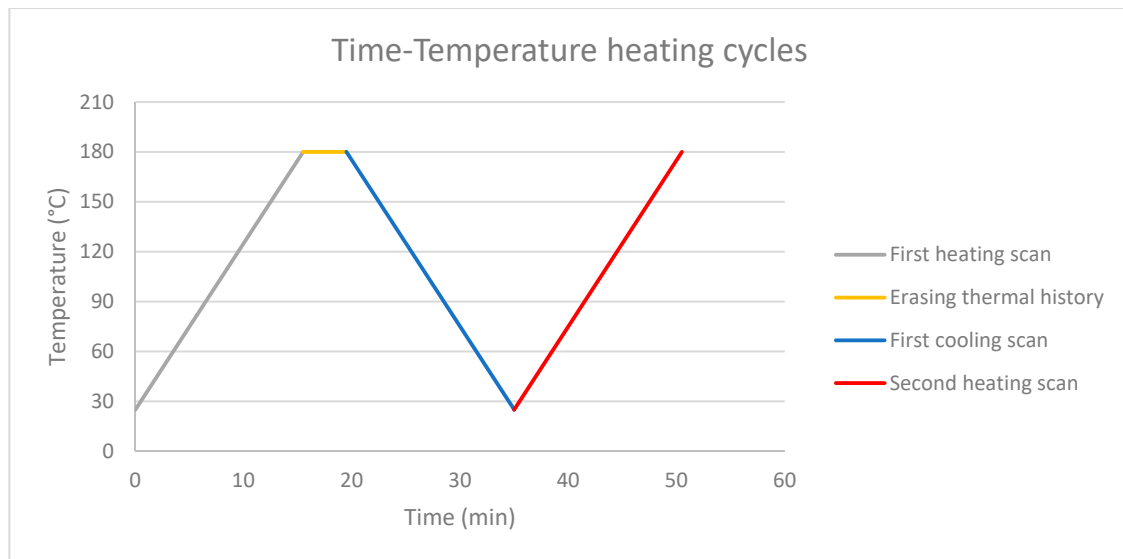


**Figure 1.** Differential Scanning Calorimetry heating cycle. Grey line is the first heating scan, yellow line is the interval to erase thermal history, blue line is the first cooling scan (evaluation of crystallization temperature  $T_c$  and crystallization enthalpy  $\Delta H_c$ ), red line is the second heating scan (evaluation of cold crystallization temperature  $T_{cc}$ , melting temperature  $T_f$  and melting enthalpy  $\Delta H_f$ ).

### 3. Results

As expected, HDPE displays no mass variation at both 35 °C and 58 °C, in agreement with literature [28], as visible from Figure 2. The addition of wood flour and recycled wastepaper influenced mass variation. Most likely, mass variation is related to natural fillers degradation, especially for wood flour addition [29]. PLA-based samples, thanks to PLA biodegradability, display mass variation, especially after three months at 58 °C.

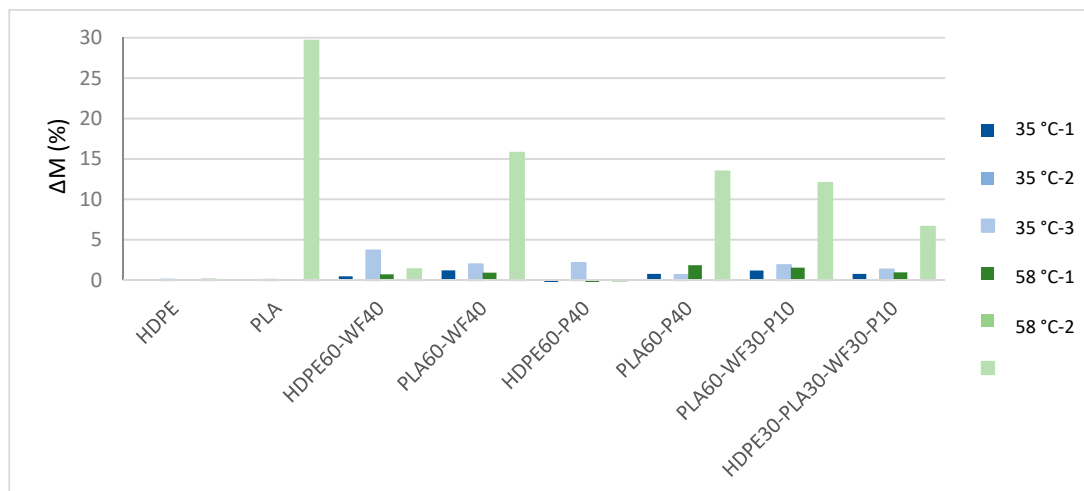


**Figure 2.** Mass variation measurements of HDPE, PLA, HDPE60-WF40, PLA60-WF40, HDPE60-P40, PLA60-P40 and PLA60-WF30-P10 for three months testing in soil at 35 °C and 58 °C.

In agreement with literature results [30], PLA is normally characterized by a first lag phase, in which diffusion of water occurs and macromolecules are still too long to be degraded by microorganisms. As a consequence, mass variation displays a higher difference for time 3 with respect to time 1 and 2. A visible effect of temperature is displayed for neat PLA degradation process. In fact, samples at 58 °C are characterized by a higher degradation rate and higher mass variation with respect to

samples at 35 °C. PLA degradation is due to breakage of ester bonds. Water hydrolyses polymer chains randomly, and as a consequence, polymer molecular weight is reduced, and oligomers are obtained. In fact, degradation can be evaluated through mass variation [31]. Wood flour and recycled wastepaper addition seems to increase mass variation for PLA-based samples at 35 °C. This can be related to humidity absorbed by wood flour and recycled wastepaper [32]. Moreover, a degradation of natural fillers can also occur, reducing sample's mass. PLA-based composites at 58 °C are characterized by a lower mass variation with respect to neat PLA. This effect could be related to increased crystallinity of PLA due to fillers addition [33]. Visual observation of samples is visible in Figure 3, and agrees with mass variation results. In fact, HDPE do not display color variation or breakage of samples. PLA buried at 35 °C displays only a lower transparency after three months buried at 35 °C, probably related to water diffusion and initial hydrolysis process, while PLA buried at 58 °C displays typical opacity for hydrolysis process already after one month, and breakage and yellowing after two and three months (Table 2).

**Table 2.** Exclusion Chromatography (SEC) results for PLA-based samples after composting tests at 35 °C and 58 °C.

	$\overline{M}_w$ (Da)						
	35 °C				58 °C		
	t0	t1	t2	t3	t1	t2	t3
PLA	41,832	41,782	45,782	44,912	35,324	8606	5083
PLA60-WF40	41,925	41,725	39,316	39,202	30,179	18,692	5334
PLA60-P40	43,283	43,052	43,576	42,529	34,934	19,898	5771
PLA60-WF30-P10	42,274	42,069	39,060	38,409	32,402	23,374	5222

Mass-average molecular weight ( $\overline{M}_w$ ) in mesophilic conditions (35 °C) did not display sensitive variations, suggesting a slow PLA degradation. In fact, the first step of PLA degradation is characterized by hydrolysis [34]. This process allows chain scissions until  $\overline{M}_w$  reach suitable chain length for microorganisms attack. Mesophilic condition seems to be insufficient to reduce PLA  $\overline{M}_w$  because of limited water diffusion and action on ester groups [35]. PLA-based composites, both with wood flour and recycled wastepaper, still display small  $\overline{M}_w$  variations. PLA-based samples tested in thermophilic conditions (58 °C), conversely, displayed  $\overline{M}_w$  sensitive reduction by time: in fact,  $\overline{M}_w$  decreased from about 40 kDa to about 5 kDa after three months. PLA degradation hydrolytic step, in agreement with literature results [36], is temperature sensitive, displaying optimal kinetic condition around 58 °C. However, recycled wastepaper seems to partially hinder PLA degradation with respect to wood flour, keeping  $\overline{M}_w$  at slightly higher values. In any case, the addition of cellulosic fillers seems to increase PLA crystallinity (considering enthalpies of PLA based samples at t0 in DSC section results), affecting water diffusion. As a consequence, a lower degradation phenomenon is displayed by composites with respect to neat PLA [37,38].

Thermogravimetric analysis has been performed on pure HDPE and on HDPE composites filled with wood flour and recycled paper, at time 0 and after 30, 60 and 90 days of composting at temperatures of 35 °C and 58 °C. Observing thermograms, the presence of fillers reduces thermal stability of samples by lowering the onset temperature degradation compared to neat HDPE, from 450 °C to 313 °C and 295 °C for recycled paper fibers and wood flour addition respectively. Low degradation temperatures of paper and wood flour are due to the presence of hemicellulose, cellulose and lignin that are sensitive to thermal degradation [27,34,35,38].

HDPE, in any case (Table 3), as reported in literature [27,34,35,38], is thermally stable up to temperatures of about 450 °C and then quickly starts to degrade, with a maximum rate of mass loss around 480 °C. Samples do not display significant variations in both onset temperature and temperature of the maximum weight variation for HDPE. The degradation leads, in all cases, to a mass loss because of thermal cracking ending around about 500 °C [32–34,36]. HDPE60-WF40 and HDPE60-P40 display

a multistep thermal degradation (Figure 4). Firstly, moisture evaporation from room temperature to about 100 °C. Secondly, thermal degradation of hemicellulose, the most thermal sensitive component in lignocellulosic fillers [39], occurs around 295 °C. Cellulose pyrolysis is displayed at higher temperature range (315–400 °C) [38–41], and at around 350 °C the maximum thermal degradation rate of cellulose and lignin is displayed. For temperatures higher than 400 °C, almost all cellulose is pyrolyzed, while lignin decomposes more slowly, over 400 °C and with a higher amount of solid residue. Samples display, considering composting progression up to time 3, a modest reduction in the initial degradation temperature with a reduction in the residual mass. HDPE60-P40, rich in cellulose, displays a residual mass approximately unchanged at around 5%, while HDPE60-WF40, due to the higher lignin content, displays higher residual mass [40]. Moreover, HDPE60-WF40 displays reduction of residual mass of samples after composting process from 11% to 7%.

**Table 3.** TGA results for HDPE and PLA based composites after three months buried at 35 °C and 58 °C. (a) Tonset results; (b) Tpeak results; (c)  $\Delta M$  results.

(a)							
	35 °C Tonset (°C)				58 °C Tonset (°C)		
	t0	t1	t2	t3	t1	t2	t3
HDPE	451	461	464	464	459	471	468
HDPE60WF40	295	295	297	297	300	291	283
HDPE60P40	313	14	304	308	305	294	298
PLA	318	333	296	324	302	258	240
PLA60WF40	296	295	293	291	296	280	248
PLA60P40	323	318	309	315	297	297	242
PLA60WF30P10	301	307	299	297	298	297	254
(b)							
	35 °C Tpeak (°C)				58 °C Tpeak (°C)		
	t0	t1	t2	t3	t1	t2	t3
HDPE	477	481	481	481	479	484	484
HDPE60WF40	356/483	350/483	340/483	336/480	341/482	351/485	333/484
HDPE60P40	344/484	346/483	336/483	346/484	333/484	326/477	320/298
PLA	343	356	320	351	336	298	271
PLA60WF40	321	314	313	313	316	306	269
PLA60P40	344	337	330	333	316	324	264
PLA60WF30P10	327	327	321	316	321	307	275
(c)							
	35 °C $\Delta M$ (%)				58 °C $\Delta M$ (%)		
	t0	t1	t2	t3	t1	t2	t3
HDPE	100	100	100	100	100	100	100
HDPE60WF40	91	89	90	93	91	91	91
HDPE60P40	95	94	95	95	93	94	93
PLA	100	100	100	100	100	100	100
PLA60WF40	89	88	88	91	90	91	96
PLA60P40	94	94	94	95	89	93	93
PLA60WF30P10	90	89	92	93	91	91	91

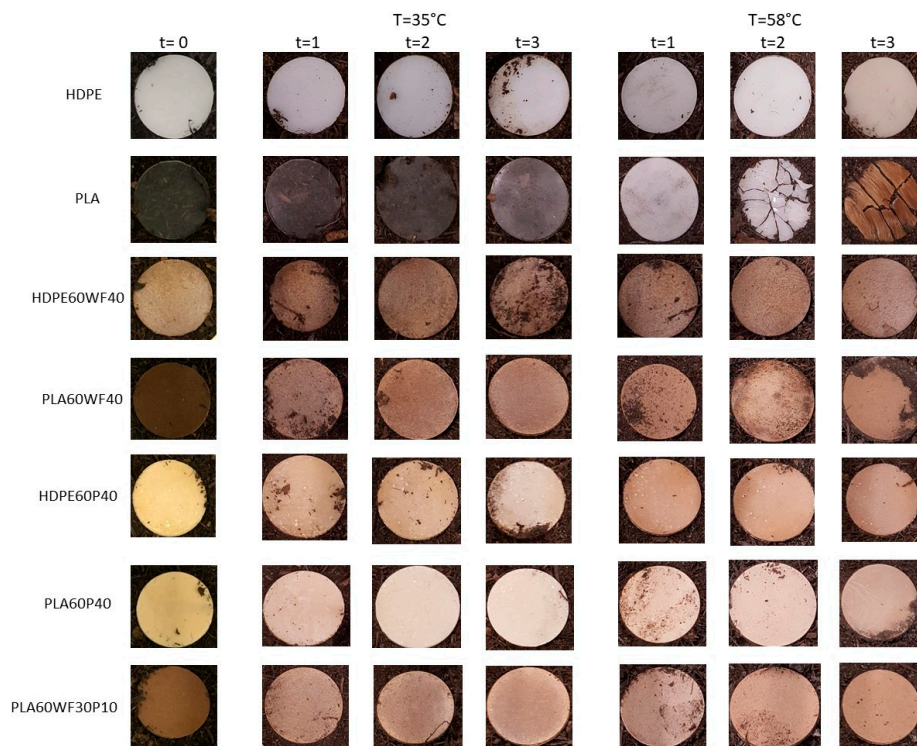


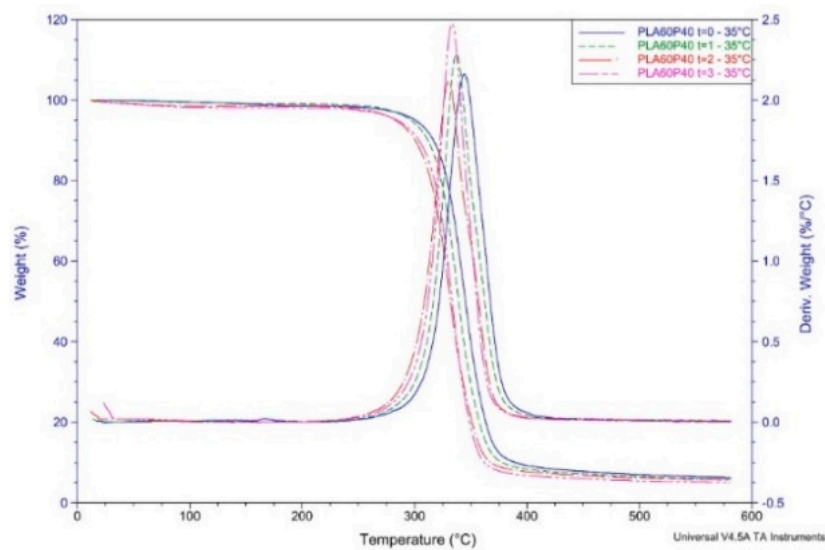
**Figure 3.** Visual observation of samples at time 0, and after 1, 2 and 3 months buried at 35 °C and 58 °C.

TGA curves of PLA display, over time, a significant difference in thermal stability between samples at 35 °C compared to 58 °C. Mesophilic conditions display a reduction of thermal stability only at time 3. Graphs display a single peak of maximum decomposition rate which starts at about 320 °C and at 350 °C. PLA is completely degraded with no residual mass. Samples after burying at 58 °C, on the other hand, display a thermal stability reduction over time, possibly related to the presence of shorter macromolecules compared to time 0, because of the degradation process [42]. The onset temperature at time 3 is about 240 °C and, at 300 °C, PLA is completely degraded with no residual mass.

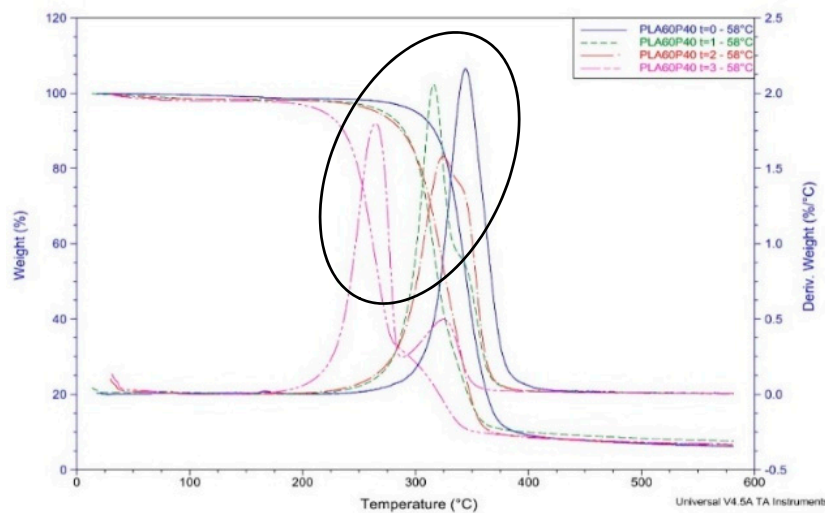
The addition of wood flour, for samples buried at 35 °C, reduces thermal stability of the composite compared to neat PLA. Samples buried at 58 °C, on the other hand, display a progressive reduction of stability over time, but higher than neat PLA. This trend is due to the hemicellulose and PLA degradation during composting process. Thermograms display that thermal decomposition of PLA60-WF40 composite occurs between 150 and 450 °C. In mesophilic and even more evident in thermophilic conditions, the presence of “shoulders” due to the overlapping of cellulose and lignin bands is highlighted. PLA, under composting conditions, displays a reduction in onset temperature degradation and sample is progressively more enriched in cellulose. As a consequence, after composting process, two separate peaks are visible, the first refers to PLA and the second to cellulose [43]. A residual mass is displayed at the end of thermal degradation, decreasing over time.

PLA60-P40 displays a reduction in thermal stability with respect to neat PLA. Thermograms display a single peak for samples buried at 35 °C, with a slight decrease in thermal stability over time. Samples at 58 °C display higher reduction of thermal stability and the appearance of shoulder, already displayed for PLA60-WF40, becomes more visible over time (Figure 4). All samples display a reduction of onset temperature with respect to PLA60-WF40, possibly associated with the lower presence of hemicellulose in paper. A residual mass is displayed at the end of thermal degradation, in a lower amount than PLA60-WF40, which remains stable over time due to the lower presence of lignin and hemicellulose [44].





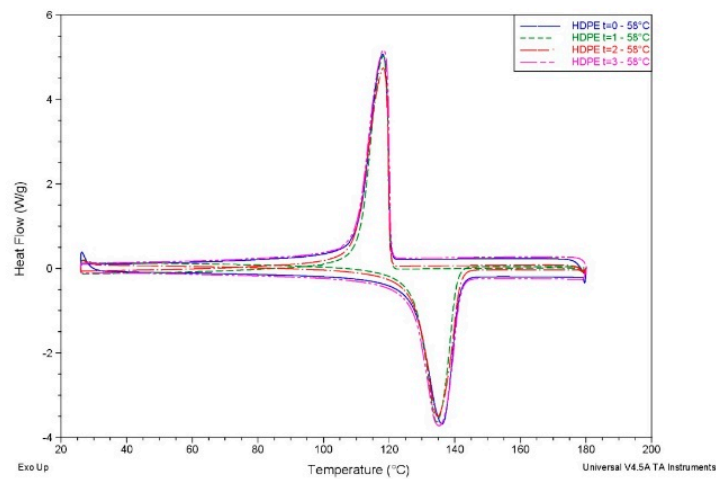
(a)



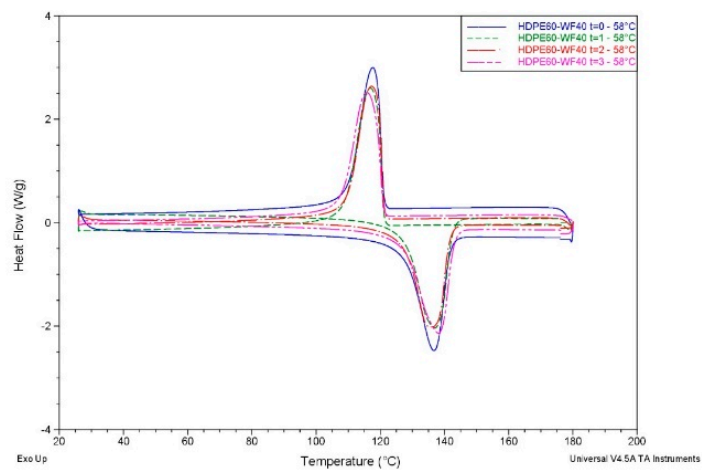
(b)

**Figure 4.** Mass loss and related peaks recorded in thermogravimetric (TG) and first order derivative of TG ascribed to the degradation of PLA60-P40 at month 0, 1, 2, 3 at 35 °C (a) and 58 °C (b).

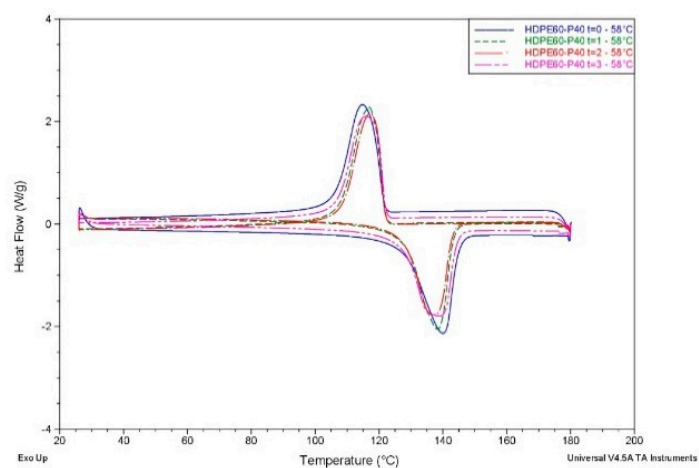
DSC analyses allow understanding of the influence of natural fillers on both HDPE and PLA thermal properties, but also the influence of composting process on materials. Neat HDPE display, as expected, no sensitive variation of melting temperature after composting at both 35 °C and 58 °C. HDPE-based composites with WF and P display higher melting and crystallization enthalpies values compared to neat HDPE. Similar observations are in agreement with results of Lee et al., who have studied the influence of different types of softwood in HDPE matrix composites [45]. This effect is more evident for P than for WF, probably because of morphological differences between P (fibrous) and WF (particulate). No sensitive variations are displayed with DSC analyses for HDPE-based samples, probably because degradation mainly occurs on natural fillers, keeping unchanged HDPE (Figure 5).



(a)



(b)



(c)

**Figure 5.** DSC thermograms for HDPE-based samples after three months buried at 58 °C: (a) neat HDPE; (b) HDPE60-WF40; (c) HDPE60-P40.

No sensitive variations have been displayed for PLA after composting at 35 °C and the curves are almost superimposable, in agreement with no mass and  $M_w$  variation. Samples after composting at 58 °C (Table 4), instead, as the composting process proceeds, show a decrease in glass transition temperature ( $T_g$ ), from 61 °C to about 40 °C after three months. Moreover, typical cold crystallization temperature ( $T_{cc}$ ) displays a decrease at 58 °C during the degradation process. This reduction may be associated with the formation of oligomers of lactic acid resulting from the cleavage of chains due to hydrolysis during composting, as confirmed also by  $M_w$  reduction. Chains with lower molecular mass crystallize more easily and have lower cold crystallization temperatures [46]. No crystallization during cooling has been detected during DSC analyses for neat PLA.

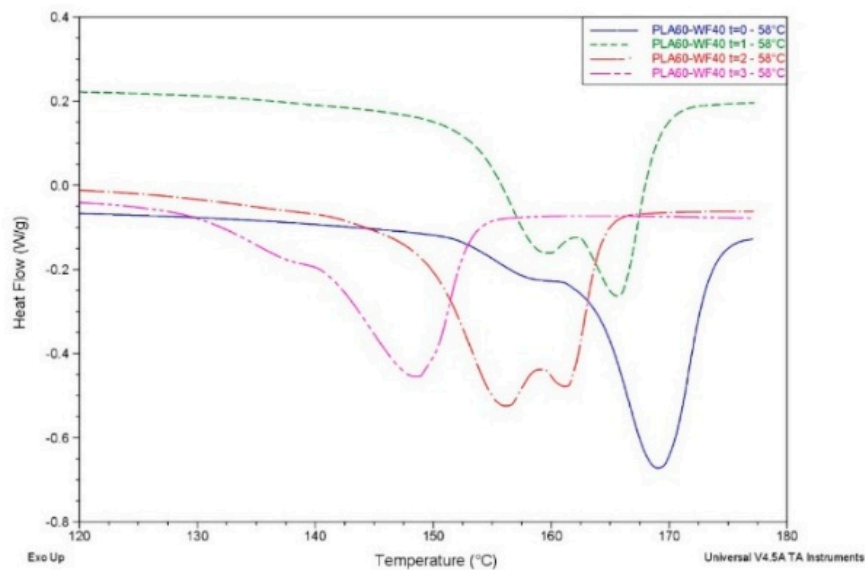
**Table 4.** DSC results for neat PLA during composting process at 58 °C.

	<b>Melting Temperature <math>T_m</math></b>	<b>Melting enthalpy <math>\Delta H_m</math> PLA</b>	<b><math>T_{cc}</math></b>	<b><math>T_g</math></b>
	(°C)	(J/gPLA)	(°C)	(°C)
PLA t0	169	48	100	61
PLA t1	166	53	94	55
PLA t2	148	47	84	45
PLA t3	144	45	90	41

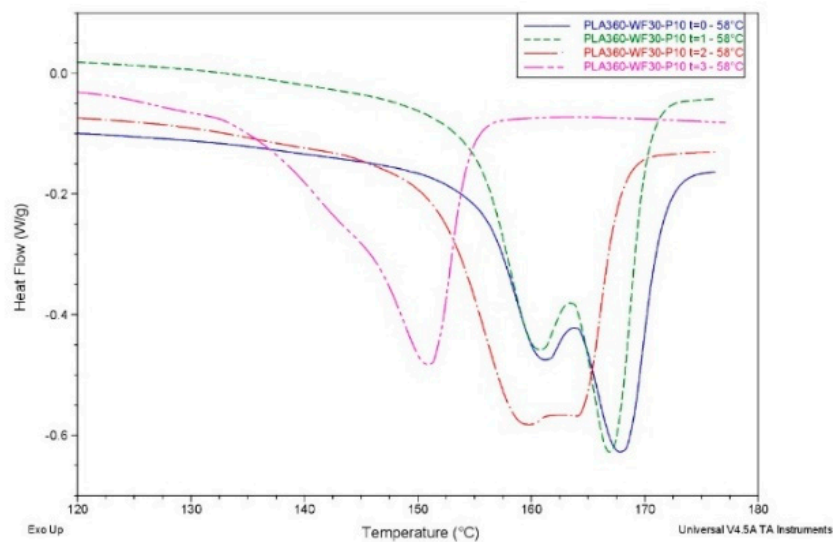
The presence of wood flour and recycled wastepaper in PLA60-WF40, PLA60-P40 and PLA60-WF30-P10 seems to be an obstacle for cold crystallization, which was not detected for these samples because of the nucleating effect of natural fillers, facilitating crystallinity from molten state. As a consequence, a formation of two melting peaks was evident (as visible from Figure 6), indicating the presence of two crystalline fractions. Moreover, thermograms of samples buried at 35 °C are almost superimposable for all composites, while at 58 °C there is a displacement of melting peaks towards lower temperatures.  $\overline{M}_w$  reduction, due to degradation progression, is responsible for  $T_g$ ,  $T_{cc}$  and  $T_m$  reduction. In fact, the lower the chain length, the easier the chain mobility [47]. In fact, under mesophilic conditions, melting temperature  $T_m$  does not show significant variations compared to neat PLA. Samples buried under thermophilic conditions display a significant reduction of  $T_m$  over time (Table 5). This reduction is analogous to the one displayed by neat PLA, and is probably associated with a decrease in  $M_w$ , although  $T_m$  of PLA-based composites are still higher than  $T_m$  of PLA.

**Table 5.** DSC results for PLA-based composites during composting process at 58 °C.

	<b><math>T_m</math></b>	<b><math>\Delta H_m</math> PLA</b>
	(°C)	(J/gPLA)
PLA60-WF40 t0	169	54
PLA60-WF40 t1	166	53
PLA60-WF40 t2	156	69
PLA60-WF40 t3	148	45
PLA60-P40 t0	171	53
PLA60-P40 t1	168	59
PLA60-P40 t2	162	62
PLA60-P40 t3	153	56
PLA60-WF30-P10 t0	168	55
PLA60-WF30-P10 t1	167	62
PLA60-WF30-P10 t2	160	69
PLA60-WF30-P10 t3	151	47



(a)



(b)

**Figure 6.** Melting peak of PLA60-WF40 (a) and PLA60-WF30-P10 (b) composites during composting process at 58 °C.

FTIR analyses validate the others obtained results, although spectra analyses would not permit quantitative comparisons. HDPE did not display any modification of its spectra after three months buried in soil at both 35 °C and 58 °C. FTIR spectra of HDPE60-P40 combine the absorption bands of HDPE matrix and characteristic absorption peaks of cellulose. Paper consists mainly of cellulose fibers but also contains hemicellulose and lignin [48]. Cellulose is characterized by a) peak at  $1425\text{ cm}^{-1}$ , known as the crystalline band, caused by the vibrations of the aromatic skeleton combined with the bending of the C–H (a lowering of its intensity reflects the decrease in the degree of crystallinity of samples), b) peak at  $1032\text{ cm}^{-1}$ , associated both with the symmetrical CO stretching of the cellulose and with the CO deformation of the primary alcohols in the lignin, c) peaks between  $3400\text{--}3300\text{ cm}^{-1}$  and  $1593\text{ cm}^{-1}$  attributed to the stretching and bending, respectively, of OH groups of cellulose [48–50]. This modification, together with the shift of peak at  $1316\text{ cm}^{-1}$  towards higher values, denotes the development of new inter- and intramolecular hydrogen bonds. The predominant degradation

phenomenon that characterizes the filler is oxidative [51], especially for hemicellulose and lignin. The oxidative process is detected by increasing intensity of the small peaks generated by the functional carbonyl group in the absorption range between 1800–1600  $\text{cm}^{-1}$ . In particular, small signals revealed in the area 1740–1709  $\text{cm}^{-1}$  are an expression of the carbonyl groups related to C=O stretching of hemicellulose groups or to the ester bond of the carboxylic group in the ferulic and coumarinic acids of the lignin and hemicellulose. This also makes this zone a good “marker” of oxidative processes; the intensity of the band around 1735  $\text{cm}^{-1}$  is usually proportional to the oxidation of hemicellulose (C=O in xylan). The areas of interest for PLA at about 1750 and 1180  $\text{cm}^{-1}$  are clearly visible, which belong to the stretching C–O and to the stretching C–O–C of PLA. Thus, 1080  $\text{cm}^{-1}$  is associated to the C–C stretching. The biodegradation of polylactic acid should determine an increase of carboxylic and alcoholic groups. There are no evident peaks variation over time at 35 °C, while at 58 °C, as the biodegradation process proceeds, PLA displays a variation related to the peak at 1750  $\text{cm}^{-1}$  due to the stretching of the C=O group. PLA biodegradation is highly sensitive to moisture, obtaining a degradation process characterized by water absorption, ester cleavage forming oligomers, solubilization of oligomer fractions and diffusion of bacteria into soluble oligomers [38]. Biodegradation of PLA should lead to an increase in carboxylic and alcoholic groups. In fact, a shift of the peak at 1750  $\text{cm}^{-1}$ , assigned to the stretching of the carbonyl, confirms a successful degradation. WF probably accelerated the degradation of composite during composting at 35 °C, over time enriched in WF. The explanation would be attributed to a greater degradation by hydrolysis of PLA due to the presence of moisture in the wood [52]. Degradation of PLA, also for PLA60-P40, can be associated with the increase of the terminal hydroxyl peak and the variation, although not always linear (probably due to the lack of homogeneity of the sample), of the peak in the area between 1730 and 1750  $\text{cm}^{-1}$ , characteristic of carbonyl groups related to C=O stretching. An increase in terminal hydroxyl peak is in agreement with a reduction in molecular mass. In conclusion, as expected, pure HDPE was non-biodegradable, while HDPE60-WF40 and HDPE60-P40 display only degradation of cellulose, lignin and hemicellulose. Neat PLA sample at 35 °C was not very sensitive to degradation processes, but biodegradation was accelerated by the presence of paper and/or wood flour. At 58 °C, pure PLA is easily biodegradable, and signs of biodegradation increase over time. PLA-based composites are characterized by PLA degradation and enrichment in cellulose, less sensitive to biodegradation.

#### 4. Conclusions

HDPE-based and PLA-based composites have been tested to analyze the effect of natural fillers (wood flour, recycled wastepaper and a mix of both fillers) on polymer degradation. Moreover, samples made of HDPE-PLA blend and a mix of two fillers have also been tested. PLA is sensitive to temperature and humidity conditions, displaying higher reduction of  $M_w$  when composting is performed at 58 °C. DSC and TGA also displayed  $T_g$ ,  $T_m$ ,  $T_{cc}$  and  $T_{onset}$  reduction after three months buried in soil. These results are in agreement with shorter macromolecules because of microorganisms attack. Natural fillers seem to influence mass variation already at 35 °C. In fact, degradation of fillers at 35 °C allows a mass reduction during composting of composites, while neat PLA do not display any variation. These results are in agreement with other analyses performed (TGA, DSC), validating natural filler degradation under composting conditions. HDPE, as expected, did not display relevant variations. A slight degradation effect is more visible for HDPE-based samples, suggesting a positive influence of natural fillers considering potential biodegradability. Future studies have to be done in order to complete the study on the effect of these fillers on HDPE and PLA composting features.

**Author Contributions:** A.Q., V.M., M.V., A.B., V.I., R.B. conceived and designed the experiments, A.Q., A.B., V.I. performed the experiments, A.Q., V.M., M.V., A.B., V.I., R.B. analyzed the data, A.Q., V.M., M.V. wrote the paper, A.B., A.Q. contributed to use of reagents/materials/analysis tools.

**Funding:** This research was funded by Bando Vinci, Erasmus project and research grant by Sapienza University of Rome.

**Conflicts of Interest:** The authors declare no conflict of interest.

## References

1. Speight, J.G. Monomers, Polymers, and Plastics. In *Handbook of Industrial Hydrocarbon Processes*; Elsevier: Oxford, UK, 2011; pp. 499–537.
2. Gajjar, C.R.; King, M.W. *Degradation Process in Resorbable Fiber-Forming Polymers for Biotextile Applications: Springer Briefs in Materials*; Springer: Basel, Switzerland, 2004.
3. Vasile, C. Role of the polymer degradation processes in environmental pollution and waste treatment. *Polimery* **2002**, *47*, 517–522. [[CrossRef](#)]
4. Kulkarni, A.; Dasari, H. Current Status of Methods Used in Degradation of Polymers: A review. *MATEC Web Conf.* **2018**, *144*, 1–11. [[CrossRef](#)]
5. Engineer, C.; Parikh, J.; Raval, A. Review on Hydrolytic Degradation Behavior of Biodegradable Polymers from Controlled Drug Delivery System. *Trends Biomater. Artif. Organs* **2001**, *25*, 79–85.
6. Tiwari, A.K.; Gautam, M.; Maurya, H.K. Recent Development of Biodegradation Techniques of Polymer. *Int. J. Res. Granthaalayah* **2018**, *6*, 414–452.
7. Gu, J.D. Microbiological deterioration and degradation of synthetic polymeric materials: Recent research advances. *Int. Biodeterior. Biodegrad.* **2003**, *52*, 69–91. [[CrossRef](#)]
8. McKew, B.A.; Dumbrell, A.J.; Taylor, J.D.; McGenity, T.J.; Underwood, G.J.U. Differences between aerobic and anaerobic degradation of microphytobenthic biofilm-derived organic matter within intertidal sediments. *FEMS Microbiol. Ecol.* **2013**, *84*, 495–509. [[CrossRef](#)] [[PubMed](#)]
9. Bajpai, M. Basics of Anaerobic Digestion Process. In *Anaerobic Technology in Pulp and Paper Industry*; Springer: Singapore, 2017; pp. 7–12.
10. Doble, M.; Kumar, A. Aerobic and Anaerobic Bioreactors. In *Biotreatment of Industrial Effluents*; Elsevier: Oxford, UK, 2005; pp. 19–38.
11. Boonmee, C.; Kositanont, C.; Leejarkpai, T. Degradation of Poly (Lactic Acid) under Simulated Landfill Conditions. *Environ. Nat. Res. J.* **2016**, *14*, 1–9.
12. Massardier, V.; Pestre, C.; Cruard-Pradet, T.; Bayard, R. Aerobic and anaerobic biodegradability of polymer films and physico-chemical characterization. *Polym. Degrad. Stab.* **2006**, *91*, 620–627. [[CrossRef](#)]
13. Arkatkar, A.S.; Arutchelvi, J.; Muniyasamy, S.; Bhaduri, S.; Uppara, P.V.; Doble, M. Approaches to Enhance the Biodegradation of Polyolefins. *Open Environ. Eng. J.* **2009**, *2*, 68–80. [[CrossRef](#)]
14. Sinclair, R.G. Blends of Polyactic Acid. Patent US5216050A, 1 June 1993.
15. As'habi, L.; Jafari, S.H.; Khonakdar, H.A.; Boldt, R.; Wagenknecht, U.; Heinrich, G. Tuning the processability, morphology and biodegradability of clay incorporated PLA/LLDPE blends via selective localization of nanoclay induced by melt mixing sequence. *Express Polym. Lett.* **2013**, *7*, 21–39. [[CrossRef](#)]
16. Quitadamo, A.; Massardier, V.; Valente, M. Interactions between PLA, PE and wood flour: effects of compatibilizing agents and ionic liquid. *Holzforschung* **2017**, *72*, 691–700. [[CrossRef](#)]
17. Quitadamo, A.; Massardier, V.; Valente, M. Optimization of Thermoplastic Blend Matrix HDPE/PLA With Different Nature and Level of Coupling Agent. *Materials* **2018**, *11*, 2527. [[CrossRef](#)] [[PubMed](#)]
18. Quitadamo, A.; Massardier, V.; Valente, M. Oil-based/Bio-Derived Thermoplastic Polymer Blends and Composites. In *Introduction to Renewable Biomaterials: First Principles and Concepts*; Lucia, L., Ayoub, A., Eds.; Wiley: Hoboken, NJ, USA, 2018; pp. 239–268.
19. Boubekour, B.; Belhaneche Bensemra, N.; Massardier, V. Valorization of waste jute fibers in developing low-density polyethylene/polylactic acid bio-based composites. *J. Reinf. Plast. Comp.* **2015**, *34*, 649–661. [[CrossRef](#)]
20. Valente, M.; Tirillò, J.; Quitadamo, A.; Santulli, S. Paper fiber filled polymer. Mechanical evaluation and interfaces modification. *Compos. Part. B-Eng.* **2017**, *110*, 520–529. [[CrossRef](#)]
21. Mohanty, A.K.; Mistra, M.; Hinrichsen, G. Biofibres, biodegradable polymers and biocomposites: An overview. *Macromol. Mater. Eng.* **2000**, *276*, 1–24. [[CrossRef](#)]
22. Gurunathan, T.; Mohanty, S.; Nayak, S.K. A review of the recent developments in biocomposites based on natural fibres and their application perspectives. *Compos. Part A-Appl. Sci. Manuf.* **2015**, *77*, 1–25. [[CrossRef](#)]
23. Rowell, R.M.; Stout, H.P. Jute and Kenaf. In *Handbook of Fibre Chemistry*; Lewin, M., Ed.; CRC Press: Boca Raton, FL, USA, 2007; Volume 3, pp. 405–452.
24. Saha, P.; Manna, S.; Roy, D.; Chowdhury, S.; Kim, K.G.; Banik, S.; Adhiikari, B.; Kim, J.K. Biodegradation of Chemically Modified Jute Fibres. *J. Nat. Fibers* **2015**, *12*, 542–551. [[CrossRef](#)]

25. Cafiero, L.; Fabbri, D.; Trinca, E.; Tuffi, R.; Vecchio Cipriotti, S. Thermal and spectroscopic (TG/DSC-FTIR) characterization of mixed plastics for materials and energy recovery under pyrolytic conditions. *J. Therm. Anal. Calorim.* **2015**, *121*, 1111–1119. [[CrossRef](#)]
26. Tuffi, R.; D'Abramo, S.; Cafiero, L.M.; Trinca, E.; Vecchio Cipriotti, S. Thermal behavior and pyrolytic degradation kinetics of polymeric mixtures from waste packaging plastics. *Express Polym. Lett.* **2018**, *12*, 82–99. [[CrossRef](#)]
27. Itavaara, M.; Karjomaa, S.; Selin, J.F. Biodegradation of polylactide in aerobic and anaerobic thermophilic conditions. *Chemosphere* **2002**, *46*, 879–885. [[CrossRef](#)]
28. Orhan, Y.; Hrenovic, J.; Buyukgungor, J.H. Biodegradation of plastic compost bags under controlled soil conditions. *Acta Chim. Slov.* **2004**, *51*, 579–588.
29. Nourbakhsh, A.; Ashori, A.; Tabrizi, A.K. Characterization and biodegradability of polypropylene composites using agricultural residues and waste fish. *Compos. Part B-Eng.* **2014**, *56*, 279–283. [[CrossRef](#)]
30. Prapruddivongs, A.; Sombatsompop, N. Biodegradation and Anti-bacterial Properties of PLA and Wood/PLA Composites Incorporated with Zeomic Anti-bacterial Agent. *Adv. Mater. Res.* **2013**, *747*, 111–114. [[CrossRef](#)]
31. Queirós, Y.G.C.; Machado, K.J.A.; Costa, J.M.; Lucas, E.F. Synthesis, characterization, and in vitro degradation of poly(lactic acid) under petroleum production conditions. *Braz. J. Pet. Gas* **2013**, *7*, 57–69.
32. Ke, T.; Sun, X. Melting behaviour and crystallization kinetics of starch and poly(lactic acid) composites. *J. Appl. Polym. Sci.* **2003**, *89*, 1203–1210. [[CrossRef](#)]
33. Mathew, A.P.; Oksman, K.; Sain, M. The effect of morphology and chemical characteristics of cellulose reinforcements on the crystallinity of polylactic acid. *J. Appl. Polym. Sci.* **2006**, *101*, 300–310. [[CrossRef](#)]
34. Ndazi, B.S.; Karlsson, S. Characterization of hydrolytic degradation of polylactic acid/rice hulls composites in water at different temperatures. *Express Polym. Sci.* **2011**, *5*, 119–131. [[CrossRef](#)]
35. Kolstad, J.K.; Vink, E.T.H.; De Wilde, B.; Debeer, L. Assessment of anaerobic degradation of Ingeo polylactides under accelerated landfill conditions. *Polym. Degrad. Stab.* **2012**, *97*, 1131–1141. [[CrossRef](#)]
36. Fortunati, E.; Luzi, F.; Puglia, D.; Dominici, F.; Santulli, C.; Kenny, J.M.; Torre, L. Investigation of thermo-mechanical, chemical and degradative properties of PLA-limonene films reinforced with cellulose nanocrystals extracted from Phormium tenax leaves. *Eur. Polym. J.* **2014**, *56*, 77–91. [[CrossRef](#)]
37. Luzi, F.; Fortunati, E.; Puglia, D.; Petrucci, R.; Kenny, J.M.; Torre, L. Study of disintegrability in compost and enzymatic degradation of PLA and PLA nanocomposites reinforced with cellulose nanocrystals extracted from Posidonia Oceanica. *Polym. Degrad. Stab.* **2015**, *121*, 105–115. [[CrossRef](#)]
38. Liu, R.; Cao, J.; Ouyang, L. Degradation of wood flour/poly (lactic acid) composites reinforced by coupling agents and organo-montmorillonite in a compost test. *Wood Fiber Sci.* **2018**, *45*, 105–118.
39. Banat, R.; Fares, M.M. Thermo-Gravimetric Stability of High Density Polyethylene Composite Filled with Olive Shell Flour. *Am. J. Polym. Sci.* **2015**, *5*, 65–74.
40. Paabo, M.; Levin, B.C. A Literature Review of the Chemical Nature and Toxicity of the Decomposition Products of Polyethylenes. *Fire Mater.* **1987**, *11*, 55–70. [[CrossRef](#)]
41. Mengeloglu, F.; Karakus, K. Thermal Degradation, Mechanical Properties and Morphology of Wheat Straw Flour Filled Recycled Thermoplastic Composites. *Sensors* **2008**, *8*, 500–519. [[CrossRef](#)] [[PubMed](#)]
42. Krehula, L.L.; Katancic, Z.; Sirocic, A.P.; Hrnjak-Murgic, Z. Weathering of high density polyethylene-wood plastic composites. *J. Wood Chem. Technol.* **2014**, *34*, 39–54. [[CrossRef](#)]
43. Yang, H.; Yan, R.; Chen, H.; Ho Lee, D.; Zheng, C. Characteristics of hemicellulose, cellulose and lignin pyrolysis. *Fuel* **2007**, *86*, 1781–1788. [[CrossRef](#)]
44. Watkins, D.; Nuruddin, M.D.; Hosur, M. Extraction and characterization of lignin from different biomass resources. *J. Mater. Res. Technol.* **2015**, *4*, 26–32. [[CrossRef](#)]
45. Kim, H.S.; Yang, H.S.; Kim, H.J.; Park, H.J. Thermogravimetric Analysis of Husk Flour Filled Thermoplastic Polymer Composites. *J. Therm. Anal. Calorim.* **2004**, *76*, 395–404.
46. Espert, A.; Camacho, W.; Karlson, S. Thermal and Thermo Mechanical Properties of Biocomposites Made from Modified Recycled Cellulose and Recycled Polypropylene. *J. Appl. Polym. Sci.* **2003**, *89*, 2353–2360. [[CrossRef](#)]
47. De Bartolo, L.; Curcio, E.; Drioli, E. *Membrane Systems: For Bioartificial Organs and Regenerative Medicine*; De Gruyter: Berlin, Germany, 2017.
48. Liao, Q.J.; Jiang, Y.C.; Turng, L.S.; Chen, C.C. Biodegradability of PLA in compost environment. In Proceedings of the SPE ANTEC, Anaheim, CA, USA, 8–10 May 2017.

49. Lee, S.H.; Wang, S. Biodegradable polymers/bamboo fiber biocomposite with biobased coupling agent. *Compos. Part A-Appl. Sci. Manuf.* **2006**, *37*, 80–91. [[CrossRef](#)]
50. Zimmermann, M.V.G.; Brambilla, V.C.; Brandalise, B.M.; Zattera, A.J. Observations of the Effects of Different Chemical Blowing Agents on the Degradation of Poly(Lactic Acid) Foams in Simulated Soil. *Mater. Res.* **2013**, *16*, 1266–1273. [[CrossRef](#)]
51. Gupta, V.K.; O'Donovan, A.; Tuohy, M.G.; Sharma, G.D. Trichoderma in bioenergy research: An overview. In *Biotechnology and Biology of Trichoderma*; Druzhinina, I., Herrera-Estrella, A., Gupta, V.K., Tuohy, M.G., Eds.; Elsevier: Amsterdam, The Netherlands, 2014.
52. Santos, R.B.; Capanema, E.A.; Balakshin, M.Y.; Chang, H.; Jameel, H. Lignin Structural Variation in Hardwood Species. *J. Agric. Food Chem.* **2012**, *60*, 4923–4930. [[CrossRef](#)] [[PubMed](#)]



© 2019 by the authors. Licensee MDPI, Basel, Switzerland. This article is an open access article distributed under the terms and conditions of the Creative Commons Attribution (CC BY) license (<http://creativecommons.org/licenses/by/4.0/>).